



An investigation of the microstructural and magnetic properties of low carbon steel processed through modified constrained studded pressing

M. M. Kaykha^a, S. S. Hosseini Faregh^{b*}, M. Khosravi^c, F. Oukati Sadeq^c

^a Department of Mechanical Engineering, Faculty of Engineering, University of Zabol

^{b*} Departments of Materials Engineering, Faculty of Engineering, Shahid Bahonar University of Kerman

^c Departments Materials Engineering, Faculty of Engineering, University of Sistan and Baluchestan

Received: 10 May 2025; Accepted: 16 June 2025

*Corresponding author, E-mail: sara_h_f@hotmail.com

ABSTRACT

The modified-constrained studded pressing (Modified-CSP) technique for improvement of the magnetic and microstructure properties of ultrafine-grain low-carbon steel sheets was investigated. The optical micrograph (OM) and scanning electron microscopy (SEM) showed that the microstructure of the samples was refined. Residual stresses and grain size of sheet samples were also investigated using X-ray diffraction (XRD) patterns. The residual stresses were increased sharply, and compressive residual stress was considered in the final pass. The vibration sample magnetometer (VSM) method was used to evaluate the magnetic properties. It was observed that the Modified-CSP method can produce low-carbon steel with ultra-fine grain and softer ferromagnetic properties.

Keywords: Severe plastic deformation, Modified-constrained studded pressing, Microstructure properties, Magnetic properties, Low carbon steel.

1. Introduction

Ultrafine-grained (UFG) materials have been widely studied by researchers due to their remarkable mechanical and physical characteristics [1,2]. Severe plastic deformation (SPD) methods involve applying intense plastic deformation to metals and alloys with coarse grains, resulting in materials with an ultrafine-grain microstructure. The main characteristic of SPD methods is that the dimensions of deformed samples remain almost constant [3,4]. Processing sheet metal and using the SPD methods is considered one of the most important industrial applications. The most commonly used SPD methods for producing ultrafine-grained or nanostructured sheet metals and alloys include constrained groove pressing (CGP) [5], repetitive corrugation and straightening (RCS) [6], the accumulative roll bonding (ARB) [8],

and the constrained studded pressing (CSP) [6]. One of the new methods recently introduced is the modified-constrained studded pressing (modified-CSP) method. One of the most significant features of this method, considering the geometry of the sample, is the application of high shear stress and the creation of residual compressive stresses [3,9]. Two possible limitations of the RCS, CGP, and CSP methods are the non-uniform strain and failure of the sheet metal during the first deformation pass. In addition, due to the accumulation of strain on the sharp edges of dies in RCS, CGP, and CSP methods, surface cracks are formed. Singh et al. [10] investigated the microstructural changes and mechanical properties of 316 austenitic stainless steel using constrained groove pressing (CGP). They observed that non-uniform strain distribution leads to uneven mechanical properties,

particularly hardness. Kumar et al. [11] applied a hybrid approach to optimizing constrained groove pressing for AA5083 sheets and low-carbon steel. Using a combination of genetic algorithm and gradient-based optimization, they improved die design, minimizing defects like unevenness and cracks, and allowing for more passes. The yield strength of AA5083 sheets increased notably after the first pass with the optimized die. Hosseini et. al [12] studied the effect of stud angle on pure copper sheets processed by constrained studded pressing (CSP) through experimental and numerical analysis. They found that a 30-degree stud angle reduced crystallite size, increased dislocation density, and resulted in improved ultimate tensile strength compared to other methods. Hosseini et. al [13] investigated the microstructure and strain distribution of pure copper sheets processed using CSP and Modified-CSP methods. All methods resulted in grain size reduction and enhanced ultimate tensile strength, with CSP using 45° studs being the most effective at reducing residual stress. CSP also led to significant grain refinement and improved overall mechanical properties. Therefore, recently, the modified-CSP method has been introduced instead of the CGP method, with the design of the optimal die profile. Therefore, to eliminate the above disadvantages, the Modified-CSP method has been used in this research as a powerful method. Despite the potential benefits of ultrafine-grained (UFG) materials, there remain significant challenges to their economic feasibility, productivity, and industrialization [1]. In addition, limited investigations were conducted on the progression of the magnetic properties of UFG metals. However, due to the widespread practical applications of sheet metal in industries such as aerospace, automotive, and electronics industries, it is very important to focus on further development of UFG materials for these purposes. The present study aims to investigate the novel application of the Modified-Constrained Studded Pressing (Modified-CSP) technique to produce ultrafine-grain low-carbon steel sheets with enhanced microstructural refinement and softer ferromagnetic properties.

2. Materials and methods

In this study, the raw material used consisted of a low-carbon steel sheet. Due to the dimensions of the dies used, the sheet samples were cut to 120×50×2 millimeters dimensions. In order to achieve a homogeneous microstructure, the sheet samples have been annealed for 1 hour at 700 °C. To apply Modified-CSP on the samples, we used the die, which is made of CK60 steel. A 30-ton hydraulic press with a constant speed of 0.05 mms⁻¹ is used for pressing. Each step of studding and flattening the

sheet was considered a separate step. Finally, eight passes were applied to the sheets. The annealed sheet, the sheet after applying one pass, and the sheet after applying eight passes were examined. The optical microscope (Olympus BH2) and field-emission scanning electron microscope (FE-SEM) (KYKY EM8000F) were used for microstructural evolution. To prepare samples for the optical microscope and scanning electron microscope, the samples were cut into dimensions of 2 × 1 × 1 mm from the center of the sheet metal samples and subsequently mounted. The samples underwent initial polishing using sandpaper with sandpaper No. Of 180, 220, 400, 800, 1500, 2000, 3000, and 3500. After that, the samples were polished at 200 rpm and etched by Nital solution (2 Vol%), with combination of 100 ml of 99.8% ethanol, 2 ml of 65% nitric acid, and distilled water. PW1730 X-ray diffractometer used for XRD analysis. The diffractometer is equipped with a copper lamp with a wavelength of 1.54 Å and an accuracy of 0.05 degrees. The XRD patterns were utilized to calculate peak areas, full width at half maximum (FWHM), and peak positions. Additionally, Warren's method was employed to determine the mean effect of line broadening. Ultimately, the XRD results were utilized to estimate the size of grains, dislocation density, and residual stress. The vibrating-sample magnetometer (VSM) test was performed by Magnetic Daghigh Kavir (MDKB) to study the magnetic properties of the samples.

3. Results and discussion

3.1. Microstructure observations

Figure 1a shows the optical micrograph of the as-received sample with a 32 μm average grain size. Figures 2 and 3 illustrate that the processes caused the average grain size to reduce to 15 μm after one pass, and reach a size in the range of ultrafine-grained after applying eight passes. One of the most important causes of the formation of ultrafine grains is the narrowing of the boundaries of dislocations. In the final pass, it can also be noted that the uniform distribution of fine grains can be noted. As seen in Figs 2a and 2b, the grains have become very fine in the first pass. In the final pass, as the intense stresses continue, not only has the average grain size become finer, but the formation of the fine and coarse grains is observed together. According to Fig. 2 b, in the sample after the eighth pass, the average grain size is gradually reduced by about 308 nm.

About the lighter phase (precipitates) visible in Fig. 2, particularly at the grain boundaries, these precipitates, observed in the scanning electron microscopy (SEM) images, are most likely carbides, such as cementite (Fe₃C), which are commonly present in low-carbon steels. These precipitates

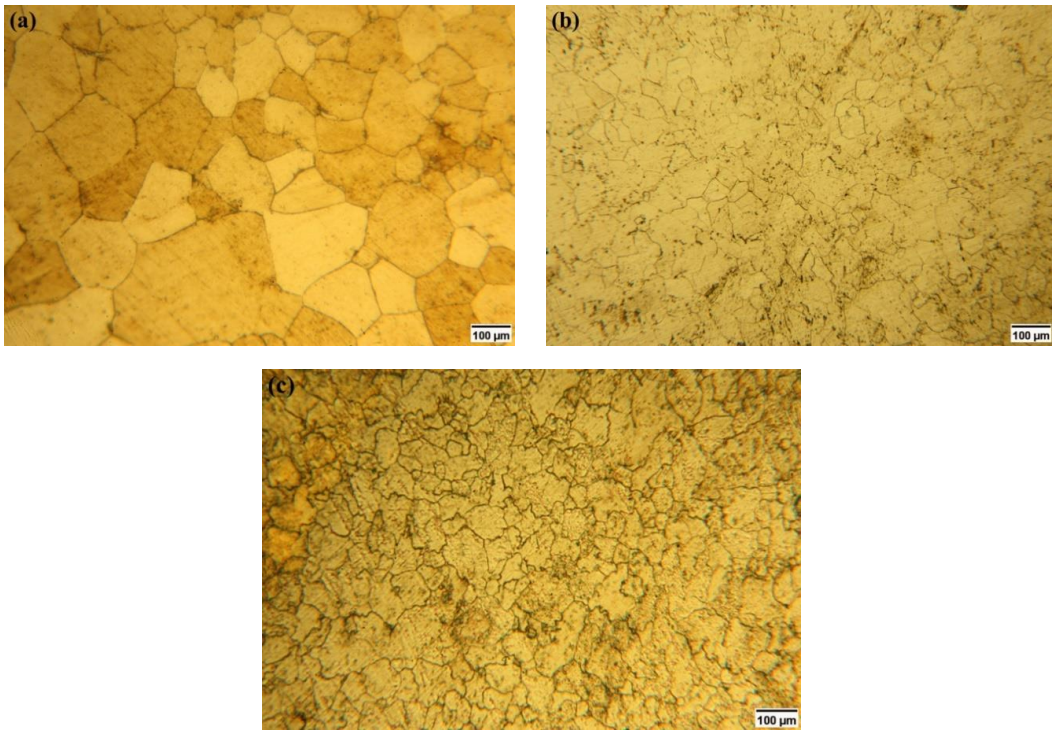


Fig. 1- Optical micrographs of samples a) as-received, b) first pass, and, c) eight pass.

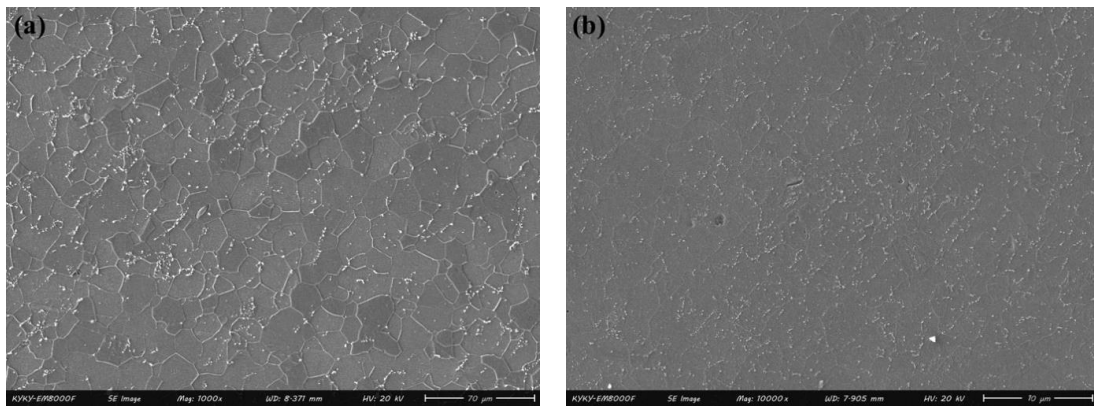


Fig. 2- FE-SEM micrograph of a) first pass and b) FE-SEM micrograph for eighth pass.

appear as brighter phases in SEM due to their higher contrast.

Given that the sample was initially annealed, it is expected that carbide precipitates (e.g., cementite) were present in the annealed microstructure, as annealing in low-carbon steels typically promotes the formation or stabilization of cementite at grain boundaries or within grains. The severe plastic deformation (SPD) process, conducted at room temperature, is unlikely to have induced the formation of new precipitates due to limited atomic diffusion at this temperature. However, the severe strain imposed during SPD may have caused fragmentation, redistribution, or accumulation of pre-existing precipitates at grain boundaries, resulting in their pronounced appearance as brighter phases in the SEM images.

This observation is supported by the work of Tsuji et al., who demonstrated that in low-carbon steels subjected to SPD, pre-existing carbide precipitates can undergo redistribution and concentrate at grain boundaries under severe strain [14].

3.2. XRD Analysis

In order to estimate the crystallite size for samples, we used the XRD pattern (Fig. 3) and the Williamson-Hall relationship. Fig. 3 shows X-ray diffraction patterns of the as-received sample, the sample after one pass, and the sample after eight passes of Modified-CSP. The XRD pattern provides evidence on the entire surface of the sample. Therefore, it was used in this study to examine the actual size of the crystallite size formed. According to calculation of crystallite size, the crystallite size after applying 1 and 8 passes of Modified-CSP is estimated to be 154 nm and 72 nm, respectively. In this article, the characteristics of the microstructure were investigated based on the peak broadening of X-ray diffraction patterns. Compared to the as-received sample, in the first and eighth passes, due to severe plastic deformation, the width of the peaks was increased. Crystallite size reduction and lattice strains in crystals are the reasons for the increasing broadening of the XRD peaks. Micro strains and grain refinement inside the crystal lattice are responsible for the increasing broadening of XRD peaks [10].

One of the important factors affecting average grain size reduction is the interaction and evaluation of dislocations with each other. Many models have been developed to clarify the annihilation and generation of dislocations during severe plastic deformation. Compared to the annealed sample, the deformed samples with the modified-CSPed technique exhibit higher dislocation density. During the first to the eighth pass of modified-CSPed, dislocation density was increased, and then average grain size and crystallite size were

decreased. During severe plastic deformation, high-angle grain boundaries (HAGBs) are formed. HAGBs stand in the way of dislocations to propagation as pinning points. Different orientations of the crystal lattice in adjacent grains need more energy for a dislocation to move across the adjacent grain. The grain boundaries are more disordered than inside the grain, which prevents the dislocations from moving in a continuous slip plane. As a result, the force required to move the dislocations increases due to their collision. Grain size reduction decreases the possible dislocation pile-up at the grain boundaries, then it increases the amount of applied stress for dislocation slip. Reduction of the grain size influences the number of dislocations at the grain boundaries. Severe plastic deformation can modify the annealed structure of HAGBs. In summary, the evaluation and interaction of dislocation densities resulting from severe plastic deformation [15] [16].

This constant rate of grain refinement is prevented by the dynamic recovery, the reactions of dislocations during deformation. Since the rate of dynamic recovery is related to the material dislocation density, straining increases the rate of dynamic recovery, which at high strains reduces the rate of grain refinement. Dynamic recovery's primary function is dislocation annihilation. Consequently, it is permissible to witness intense grain refinement during the first passes of Modified-CSP and a decreased refinement rate during subsequent passes [17].

In this study, for the as-annealed sample, the grain size reported in Table 1 is based on the average grain size determined using microscopy techniques (e.g., optical microscopy (OM) and scanning electron microscopy (SEM)) in accordance with ASTM E112 (linear intercept method). Thus, the grain size for this sample was not solely derived from XRD analysis but was obtained through microscopy to ensure greater accuracy. For the first-pass and eighth-pass samples, XRD was used as a complementary method to estimate crystallite sizes. Notably, for the eighth-pass sample, which exhibits a nanostructured microstructure due to severe plastic deformation (SPD), XRD is a reliable and appropriate method, and its results are consistent with microscopy observations.

Regarding dislocation density, the values reported in Table 1 were calculated based on the methodology outlined in the referenced work by Ungár et al., which utilizes XRD peak broadening analysis to estimate dislocation density in deformed materials. This approach is well-suited for SPD-processed samples (e.g., first and eighth passes) and was applied to the as-annealed sample as a preliminary estimation, consistent with the observed microstructural trends [18].

3.3. Residual stresses

Plastic deformation leads to create residual stresses. Changes in residual stresses and crystallite size were calculated using XRD pattern analysis. The residual stresses are in equilibrium with the environment, so the amount and type are very important. XRD analysis is a non-destructive technique for studying residual stress. The basis of this method is to measure the distance between parallel crystalline planes. The presence of residual stress in the workpiece causes changes in the distance between crystal planes, which in turn alter the angle of diffraction of X-rays. This method is based on measuring the distance between parallel crystal planes [20]. The most

common method of measurement of residual stress is $\text{Sin}^2\psi$.

Fig. 4 displays the XRD patterns versus 2θ angle for low carbon steel, first and eighth passes of Modified-CSP samples. Residual stress changes from -759 MPa for the as-received to -2313 MPa for the first-pass samples. When the number of passes increased, in the final pass, the amount of compressive residual stress was -3807 MPa. Increasing the number of passes causes to increase in the peak broadening, which indicates the average grain size reduction. The origin of the residual stresses is heterogeneous plastic deformation on the macroscopic and microscopic scale of the material; therefore, with increasing

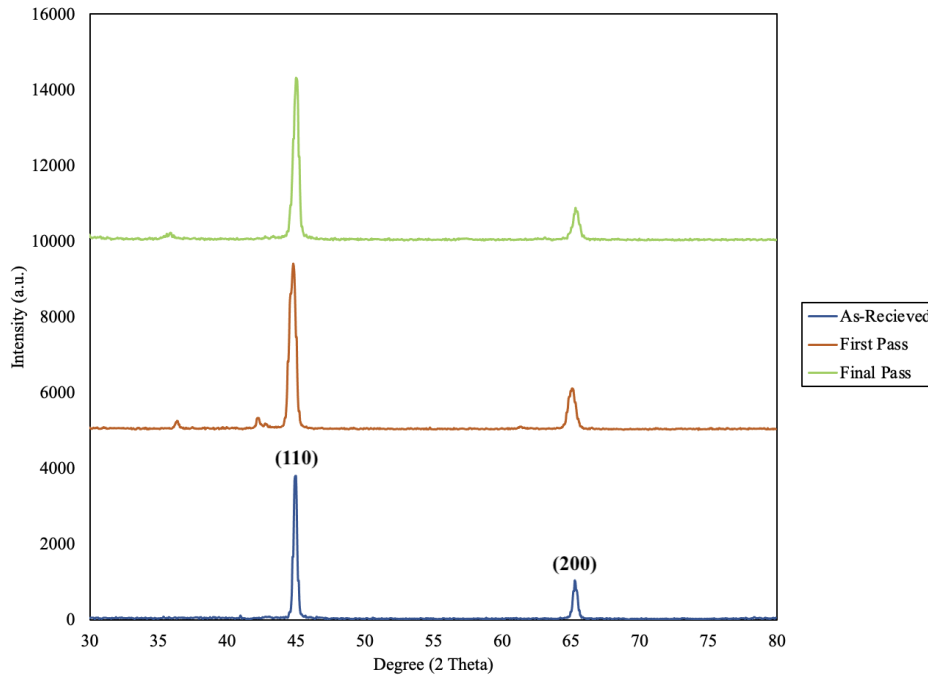


Fig. 3- X-ray diffraction patterns of as received, first, and final passes.

Table. 1- Grain size and density of dislocations in as-annealed, the first, and eighth pass samples *[19]

Pass No.	Average grain size(nm)	Crystallite size (nm)	ρ (1/nm ²)
As received	32000	32000	0.0017*
1	15000	154	2.58
8	308	72	14.1

effective plastic strain applied at higher passes and uniformity of strain distribution, the residual values are greatly increased. Fatigue life is reduced by tensile residual stresses. It is postponed by the compressive residual stresses on the surface of the parts, to prevent cracks formation and propagation [21]. Likewise, the performance of compressive residual stresses improves the wear resistance and corrosion of materials [22].

3.4. VSM Analysis

One of the most crucial properties of alloys and metals that is influenced by plastic deformation is their magnetic properties. A vibration sample magnetometer (VSM) can be used as a test for evaluating the magnetic characteristics of metallic materials. Fig. 5 presents the Vibrating Sample Magnetometry (VSM) results for low-carbon steel samples in both deformed and undeformed conditions. Additionally, Fig. 6 provides a comparative analysis of key magnetic parameters, including saturation magnetization (M_s), residual magnetization (M_r), and coercivity (H_c), for the investigated samples.

As depicted in Fig. 5 and Fig. 6, an increase in plastic deformation leads to an enhancement in the M_s . This phenomenon can be attributed to the introduction of additional defects, such as grain boundaries and dislocations, due to plastic deformation. These defects can enhance the number of magnetic domains and facilitate

their alignment, thereby increasing the saturation magnetization (M_s). Consequently, this effect increases the magnetic moments per unit volume, leading to a rise in saturation magnetization (M_s). Furthermore, plastic deformation alters the microstructural characteristics, including grain size and shape. A reduction in grain size increases the number of grain boundaries, which act as nucleation sites for magnetic domains. This, in turn, enhances the magnetic moments per unit volume and contributes to the observed increase in saturation magnetization [23, 24].

Moreover, Figs. 5 and 6 indicate a reduction in coercivity (H_c) with increasing plastic deformation. This decrease in H_c may be attributed to several factors. One possible explanation is that plastic deformation introduces a high density of dislocations within the material, leading to defects and distortions in the crystal lattice structure. These structural modifications can influence domain wall motion, reducing the energy required for magnetization reversal and consequently lowering the coercivity. These defects can serve as nucleation sites for magnetic domain formation, thereby promoting domain generation and contributing to the reduction in coercivity (H_c). Additionally, plastic deformation induces residual stresses that influence the magnetic properties of the material. These stresses can modify magnetic anisotropy and lower the energy barrier for magnetic domain wall movement, facilitating domain motion and further

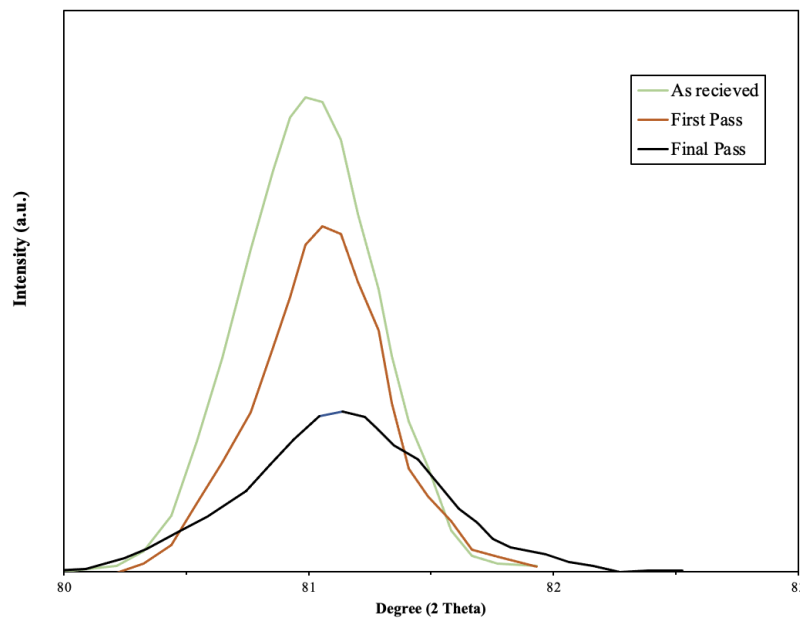


Fig. 4- XRD patterns for residual stress (a) as received, (b) first, and (c) final passes samples.

decreasing H_c . Moreover, severe plastic deformation can significantly alter the microstructure, including grain size and morphology, which in turn affects the magnetic behavior. For instance, a reduction in grain size increases the number of grain boundaries and decreases the size of magnetic domains, allowing for easier domain motion and leading to a further decrease in H_c [25, 26].

4. Conclusions

In this study, low-carbon steel sheets were subjected to severe plastic deformation using the Modified-CSP technique for up to eight passes. The effects on microstructure, residual stress, and magnetic properties were investigated through experimental methods, including XRD and VSM analyses. The key findings are as follows:

1. The Modified-CSP process produced ultrafine-grained steel sheets with uniform grain distribution and increased dislocation density.
2. XRD analysis confirmed grain refinement

and higher dislocation densities as deformation increased.

3. The average grain size was reduced from 15 μm after the first pass to 308 nm after the eighth pass, while dislocation density increased from 0.2765 to 1.0032 ($1/\text{nm}^2$).

4. Compressive residual stress increased from -759 MPa (annealed) to -3807 MPa (eighth pass), indicating significant strain hardening.

5. Increased compressive stress and uniform strain distribution can enhance fatigue life, wear resistance, and corrosion resistance.

6. The refined grain structure improved magnetic properties, including higher saturation magnetization and reduced coercivity and hysteresis losses.

7. Overall, the MCSP technique effectively enhanced the mechanical and magnetic performance of low-carbon steel by inducing grain refinement, dislocations, and beneficial residual stresses.

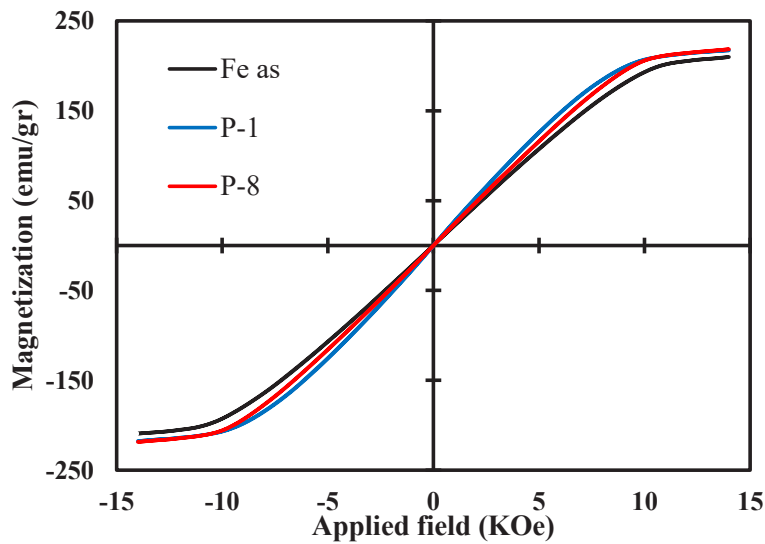


Fig. 5- VSM test of deformed and as-received samples.

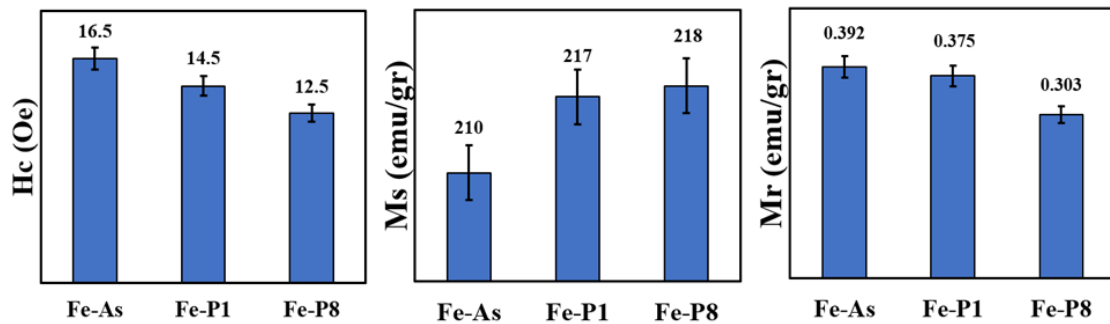


Fig. 6- The saturation magnetization (M_s), residual magnetization (M_r), and coercivity (H_c) of different samples.

References

1. Zangiabadi, A. and M. Kazeminezhad, Development of a novel severe plastic deformation method for tubular materials: Tube Channel Pressing (TCP). *Materials Science and Engineering: A*, 2011. 528(15): p. 5066-5072.
2. Mirzadeh, H, Superplasticity of fine-grained austenitic stainless steels: A review. *Journal of Ultrafine Grained and Nanostructured Materials*, 2023. 56(1): p. 27-41.
3. Kaykha, M.M. and M.R. Dashtbayazi, An Improvement in constrained studded pressing for producing ultra-fine-grained copper sheet. *Metals*, 2022. 12(2): p. 193.
4. Izi, A. Honarpisheh, M. Ahmadi, F, Non-Uniform Simple Shear Extrusion(NUSSE) Technique as a novel sever plastic deformation technique. *Journal of Ultrafine Grained and Nanostructured Materials*, 2024. 57: p. 9.
5. Shin, D.H., et al., Constrained groove pressing and its application to grain refinement of aluminum. *materials Science and Engineering: A*, 2002. 328(1-2): p. 98-103.
6. Zhu, Y.T., et al., A new route to bulk nanostructured metals. *Metallurgical and Materials Transactions*, 2001. 32(6): p. 1559-1562.
7. Saito, Y., et al., Ultra-fine grained bulk aluminum produced by accumulative roll-bonding (ARB) process. *Scripta materialia*, 1998. 39(9): p. 1221-1227.
8. Torkestani, A. and M. Dashtbayazi, A new method for severe plastic deformation of the copper sheets. *Materials Science and Engineering: A*, 2018. 737: p. 236-244.
9. Kaykha, M. and M. Dashtbayazi, Experimental and numerical investigation of severe plastic deformation of copper sheets processed by modified-constrained studded pressing. *Materials Research Express*, 2022. 9(1): p. 016523.
10. Singh, R., et al., Microstructural evolution and mechanical properties of 316 austenitic stainless steel by CGP. *Materials Science and Engineering: A*, 2021. 812: p. 141105.
11. Kumar, S., K. Hariharan, and R. Digavalli, Hybrid optimization of die design in constrained groove pressing. *Materials and Manufacturing Processes*, 2020. 35(6): p. 687-699.
12. Hosseini Faregh, S., R. Raiszadeh, and M. Dashtbayazi, Pure Copper Sheets Processed by Constrained Studded Pressing: The Effect of Die Angle. *Journal of Materials Engineering and Performance*, 2023: p. 1-11.
13. Faregh, S.H., R. Raiszadeh, and M. Dashtbayazi, Comparing the Microstructure and Mechanical Properties of Pure Copper Sheets Subjected to Different Types of Constrained Dies Pressing. *Transactions of the Indian Institute of Metals*, 2024. 77(3): p. 727-735.
14. Tsuji, N., Strength and ductility of ultrafine grained aluminum and iron produced by ARB and annealing. *Materials Science and Engineering A*, 350, 2002, (108-116).
15. Valiev, R.Z. and T.G. Langdon, Principles of equal-channel angular pressing as a processing tool for grain refinement. *Progress in materials science*, 2006. 51(7): p. 881-981.
16. Krishnaiah, A., U. Chakkingal, and P. Venugopal, Production of ultrafine grain sizes in aluminium sheets by severe plastic deformation using the technique of groove pressing. *Scripta Materialia*, 2005. 52(12): p. 1229-1233.
17. F. Khodabakhshi, M. Kazeminezhad, A.H. Kokabi, Constrained groove pressing of low carbon steel: Nano-structure and mechanical properties. *Materials Science and Engineering, A* 527 (2010), 4043-4049.
18. Ungár, T, The effect of dislocation contrast on x-ray line broadening: A new approach to line profile analysis. *Journal of Applied Crystallography*, 34, 2001, 298-310.
19. K Horiuchi, T Ogawa, Z Wang, Y Wang, Y Adachi, Three-dimensional analysis of ferrite grains recrystallized in low-carbon steel during annealing. *Materials*, 2021.
20. Prevéry, P.S., X-ray diffraction characterization of residual stresses produced by shot peening. *Shot Peener(USA)*, 2001. 15(1): p. 4-8.
21. Totten, G.E., *Handbook of residual stress and deformation of steel*. 2002: ASM international.
22. Rossini, N., et al., Methods of measuring residual stresses in components. *Materials & Design*, 2012. 35: p. 572-588.
23. Sablik, M., Modeling the effect of grain size and dislocation density on hysteretic magnetic properties in steels. *Journal of Applied Physics*, 2001. 89(10): p. 5610-5613.
24. Reekie, J. and T. Hutchison, The Effect of Cold Working on the Magnetic Properties of Pure Metals. *Physical Review*, 1948. 74(5): p. 610.
25. Stupakov, O., et al., Investigation of magnetic response to plastic deformation of low-carbon steel. *Materials Science and Engineering: A*, 2007. 462(1-2): p. 351-354.
26. Kuleev, V., T. Tsar'kova, and A. Nichipuruk, Effect of tensile plastic deformations on the residual magnetization and initial permeability of low-carbon steels. *Russian Journal of Nondestructive Testing*, 2006. 42: p. 261-271.